A multiplier peroxiporin signal transduction pathway powers piscine spermatozoa

François Chauvigné[a], Carla Ducat[a], Alba Ferré[a], Tom Hansen[b], Montserrat Carrascal[c], Joaquín Abián[c], Roderick Nigel Finn[a,d], and Joan Cerdà[a,1]

[a]Institute of Agrifood Research and Technology, Institute of Biotechnology and Biomedicine, Universitat Autònoma de Barcelona, 08193 Barcelona, Spain; [b]Institute of Marine Research, Matre Aquaculture Research Station, 5984 Matredal, Norway; [c]Consejo Superior de Investigaciones Cientificas/Universitat Autònoma de Barcelona Proteomics Laboratory, Instituto de Investigaciones Biomédicas de Barcelona-Consejo Superior de Investigaciones Cientificas-August Pi i Sunyer Biomedical Research Institute, 08193 Barcelona, Spain; and [d]Department of Biology, Bergen High Technology Centre, University of Bergen, 5020 Bergen, Norway

Edited by Mariana F. Wolfner, Cornell University, Ithaca, NY, and approved January 26, 2021 (received for review September 17, 2020)

The primary task of a spermatozoon is to deliver its nuclear payload to the egg to form the next-generation zygote. With polyandry repeatedly evolving in the animal kingdom, however, sperm competition has become widespread, with the highest known intensities occurring in fish. Yet, the molecular controls regulating spermatozoon swimming performance in these organisms are largely unknown. Here, we show that the kinematic properties of postactivated piscine spermatozoa are regulated through a conserved trafficking mechanism whereby a peroxiporin ortholog of mammalian aquaporin-8 (Aqp8bb) is inserted into the inner mitochondrial membrane to facilitate H_2O_2 efflux in order to maintain ATP production. In teleosts from more ancestral lineages, such as the zebrafish (*Danio rerio*) and the Atlantic salmon (*Salmo salar*), in which spermatozoa are activated in freshwater, an intracellular Ca^{2+}-signaling directly regulates this mechanism through monophosphorylation of the Aqp8bb N terminus. In contrast, in more recently evolved marine teleosts, such the gilthead seabream (*Sparus aurata*), in which spermatozoa activation occurs in seawater, a cross-talk between Ca^{2+}- and oxidative stress-activated pathways generate a multiplier regulation of channel trafficking via dual N-terminal phosphorylation. These findings reveal that teleost spermatozoa evolved increasingly sophisticated detoxification pathways to maintain swimming performance under a high osmotic stress, and provide insight into molecular traits that are advantageous for postcopulatory sexual selection.

aquaporin | mitochondria | sperm | oxidative stress | sexual selection

For many dioecious animals, spermatozoon velocity, progressivity, and duration of motility are vital determinants of reproductive success and are thus major selection criteria for sperm evolution (1–6). Maximizing such kinematic properties contributes to spermatozoon vigor (7); however, due to the limitations in sperm ATP stores, which provide the chemical energy for flagellar contractions, a trade-off between swimming fast and for extended periods typically exists (8). Optimal combinations of traits that improve spermatozoon vigor are nevertheless important in polyandrous vertebrates facing sperm competition, which represents a powerful form of postcopulatory sexual selection (9–15). Since the phenomenon of sperm competition was first recognized (16), investigators have sought to understand the underlying mechanisms that could explain advantageous trait selection (17). To date, however, most research has focused on the physical and morphological properties involved in sperm competition, and very little is known concerning the molecular and genetic mechanisms underpinning spermatozoon performance (15, 18, 19).

One positively selected morphological change in respect of spermatozoon velocity and longevity in vertebrates as diverse as fishes, birds, and mammals, has been the increase in the spermatozoon midpiece size and the number or scale of mitochondria therein (20–22). Such changes have logically been associated with increased mitochondrial production of ATP for improved flagellar motility. However, the biochemical reactions that lead to increased ATP synthesis also generate elevated levels of hydrogen peroxide (H_2O_2), a reactive oxygen species (ROS) that inhibits mitochondrial function and suppresses flagellar motility (23–27). With osmotic stress of the exposed ejaculate generating additional ROS (26, 28), it has been unclear how sperm evolved molecular mechanisms that surmount such signaling conflicts.

A solution to this apparent paradox was recently discovered in the spermatozoa of a marine teleost, in which a water channel protein, now termed Aqp8bb (a peroxiporin ortholog of mammalian aquaporin-8) (29), is rapidly (<1 s) trafficked to the inner mitochondrial membrane upon activation in seawater (SW) to facilitate H_2O_2 efflux and the maintenance of ATP production and flagellar motility (26). The importance of Aqp8bb, which mainly functions as a peroxiporin in these germ cells, was demonstrated through immunological inhibitory experiments, which highlighted the channel-trafficking mechanism as a critical regulator of the spermatozoon velocity and motility (26). To date, however, the signal transduction pathways that regulate peroxiporin trafficking in vertebrate spermatozoa remain completely unknown.

Among externally fertilizing vertebrates, the highest known intensity of sperm competition occurs in true bony fishes (teleosts) (6), and we therefore focused our investigations on these model organisms. In contrast to amniotic vertebrates, in which ejaculates become gelatinous when emitted (30), the ejaculates

Significance

Spermatozoon swimming performance is critical for fertilization success in fishes, yet the cellular mechanisms that regulate this vital trait are poorly understood. Here, we discovered that a water channel protein, acting as an H_2O_2 channel (peroxiporin) to detoxify the mitochondria, directly regulates the velocity and progressive motility of both freshwater and marine spermatozoa. The mitochondrial insertion of the peroxiporin is controlled by an increasingly sophisticated hierarchy of intracellular signaling cascades, which evolved into a multiplier stress-activated pathway in modern marine species. These adaptive solutions maximize the postactivated swimming performance of sperm under conditions of high osmotic and oxidative stress. Our findings thus reveal that the pathways regulating the peroxiporin transport in fish spermatozoa provide an advantage for competitive fertilization success.

Author contributions: F.C. and J.C. designed research; F.C., C.D., A.F., and T.H. performed research; T.H., M.C., and J.A. contributed new reagents/analytic tools; F.C., R.N.F., and J.C. analyzed data; and F.C., R.N.F., and J.C. wrote the paper.

The authors declare no competing interest.

This article is a PNAS Direct Submission.

[1]To whom correspondence may be addressed. Email: joan.cerda@irta.cat.

This article contains supporting information online at https://www.pnas.org/lookup/suppl/doi:10.1073/pnas.2019346118/-/DCSupplemental.

Published March 4, 2021.

of freshwater (FW) and marine teleosts are not only rapidly diluted, but respectively face tremendous and opposing osmotic stresses, which in most species activate sperm motility (31–33). To understand the significance of such harsh environments for peroxiporin signal transduction pathway evolution, we selected model species from ancient and modern lineages of teleosts, including the FW ostariphysan zebrafish (*Danio rerio*), the FW protacanthopterygian Atlantic salmon (*Salmo salar*), and the modern marine acanthomorph gilthead seabream (*Sparus aurata*). Using a combination of pharmacological, molecular, and physiological approaches, we uncover the evolution of increasingly sophisticated peroxiporin signal transduction pathways powering their spermatozoa. The findings provide insight into the underlying hierarchy of systemic molecular traits that regulate the velocity, progressivity and duration of spermatozoon motility.

Results

Activated Piscine Spermatozoa Traffic the Aqp8bb Peroxiporin to Mitochondria. To investigate whether Aqp8bb is trafficked to the mitochondria of activated spermatozoa of FW teleosts as observed in the marine gilthead seabream (26), we first confirmed that the Aqp8bb orthologs of Atlantic salmon and zebrafish are expressed in intratesticular and ejaculated spermatozoa (*SI Appendix*, Figs. S1 and S2). Immunofluorescence microscopy of sperm maintained in the corresponding nonactivating medium (NAM), previously loaded with the mitochondrion-specific vital dye MitoTracker Red CMXRos (MTR), and using species-specific affinity-purified Aqp8bb antibodies, showed that the seabream Aqp8bb peroxiporin was distributed in the midpiece region and anterior part of the flagellum in immotile sperm, whereas in salmon and zebrafish Aqp8bb was mostly located in more discrete areas surrounding the spermatozoon head (Fig. 1 *A*–*C*). Upon SW- (seabream) or FW- (salmon and zebrafish) activation of sperm motility, Aqp8bb was rapidly accumulated in the mitochondria of each species (Fig. 1 *A*–*C*). Quantification of immotile and motile spermatozoa showing colocalization of Aqp8bb and MTR signals indicated that >75% of activated spermatozoa from each species showed Aqp8bb mitochondrial accumulation (Fig. 1 *D*–*F*), revealing that the peroxiporin trafficking mechanism during sperm motility is a conserved trait in teleosts.

Signaling Pathways Involved in Aqp8bb Intracellular Trafficking in SW Spermatozoa. To uncover the signaling pathways involved in the Aqp8bb trafficking mechanism of seabream spermatozoa, we used a battery of protein kinase inhibitors and activators (Fig. 2 and *SI Appendix*, Table S1). Immunofluorescence microscopy and immunoblotting data showed that the transit of Aqp8bb to the SW-activated sperm mitochondrion was strongly inhibited in a dose-dependent manner by the JNK inhibitor SP600125 with respect to spermatozoa treated with dimethyl sulfoxide (DMSO) vehicle (control), whereas CHIR99021 and BIM-II, typical blockers of glycogen synthase kinase 3 (GSK3) and protein kinase C (PKC), respectively, also reduced Aqp8bb transport but were less effective (Fig. 2 *A* and *B*). In contrast, inhibitors of p38 mitogen-activated protein kinase (p38 MAPK) and protein kinase A (PKA), such as SB202190 and BIRB796, and H-89, respectively, showed no effect (Fig. 2 *A* and *B*). We further tested the effect of inhibitors of several JNK upstream regulators, including the MAPKKKs MAP3K7/TAK1, germinal center kinases (GCKs), apoptosis signal-regulating kinase 1 (ASK1), and mitogen-activated protein kinase kinases (MKKs) (34), on Aqp8bb trafficking, using the compounds NG25, GNF-7, NQDI-1, and PD98059. The data indicated that only ASK1 and MKKs inhibitors can reduce Aqp8bb mitochondrial accumulation in a dose-dependent manner (Fig. 2 *A* and *B*), suggesting that a canonical ASK1-MKK-JNK cascade, as well as PKC and GSK3 signaling pathways, regulate Aqp8bb trafficking in activated seabream spermatozoa.

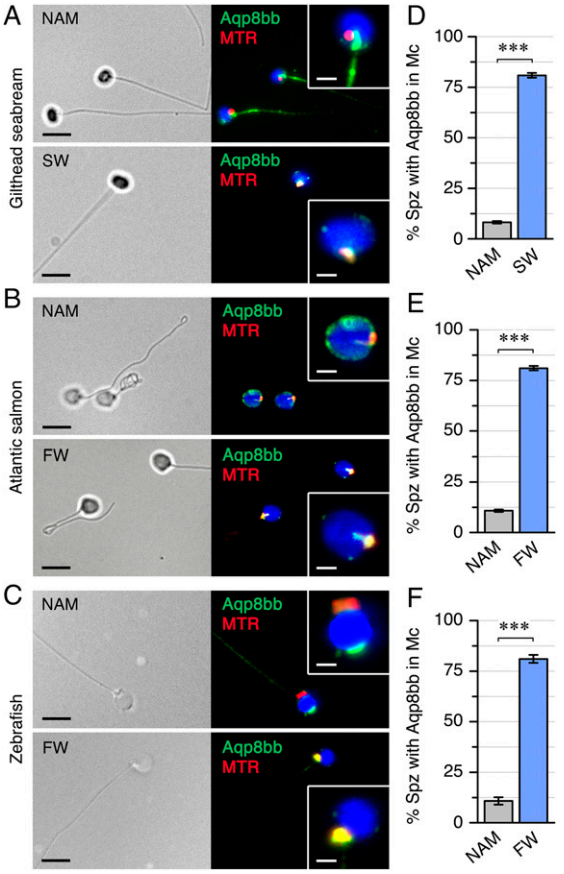

Fig. 1. The piscine Aqp8bb peroxiporin is transported to the mitochondria during spermatozoon motility activation. (*A*–*C*) Representative bright field images (*Left*) and immunodetection (*Right*) of Aqp8bb (green) in immotile (diluted in NAM) and activated spermatozoa of SW and FW spawning teleosts, using species-specific Aqp8bb antibodies. The mitochondria are labeled with MTR (red), whereas the spermatozoa nucleus are counterstained with DAPI (blue). Colocalized signals in mitochondria are yellow. (Scale bars, 5 μm; *Insets*, 1 μm.) (*D* and *F*) Percentage of spermatozoa showing Aqp8bb mitochondrial localization after incubation in NAM or upon activation in SW or FW in each species. Data are the mean ± SEM ($n = 4$ to 5 fish in *D* and *E*, and $n = 3$ pools of 5 different males each in *F*). Significance was measured by an unpaired Student's *t* test with respect to immotile sperm. ***$P < 0.001$.

Immunoblotting experiments confirmed the expression of ASK1, MKK4, JNK, and GSK3α/β kinases in immotile seabream spermatozoa (*SI Appendix*, Fig. S3*A*). Upon the hyperosmotic shock in SW, the phosphorylation of MKK4^{T261}, JNK$^{T183/Y185}$, and GSK3α/β$^{Y279/216}$ increased, whereas the inhibitory phosphorylation of ASK1^{S966} and GSK3α^{S21} decreased, suggesting that the catalytic activities of all of these kinases are activated (35–37). The inhibitory phosphorylation of GSK3β^{S9} seems not to be involved during seabream sperm activation, since phosphorylated GSK3β^{S9} was detected in testis extracts but not in spermatozoa (*SI Appendix*, Fig. S3*B*). Phosphorylation of JNK$^{T183/Y185}$ in SW-activated sperm was not affected by inhibitors of JNK, p38 MAPK, PKA, or GSK3 kinetic activity (Fig. 2*C*). However, JNK$^{T183/Y185}$ phosphorylation was reduced by PKC inhibition, although not completely, whereas that of Gsk3α/β$^{Y279/216}$ was partially decreased by both PKC and JNK blockage (Fig. 2*C*). Upon SW activation, the respective inhibition of the JNK upstream kinases ASK1 and MKK4 decreased MKK4^{T261}, JNK$^{T183/Y185}$, and GSK3α/β$^{Y279/216}$ phosphorylation (Fig. 2*C*), which is in accordance with the known role of ASK1 phosphorylating MKK4 (34) and the ability of PD98059 to prevent MKKs activation (38). Together, these data suggest that the ASK1-MKK4-JNK

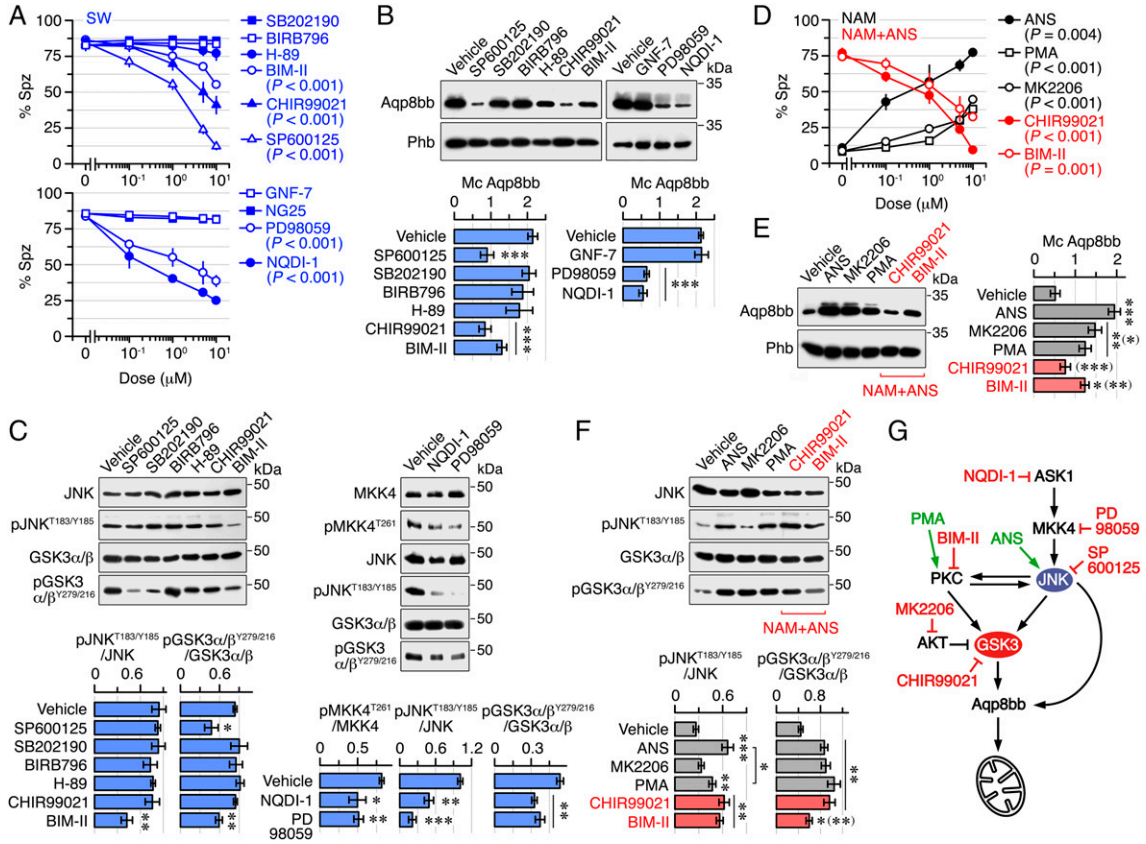

Fig. 2. Pharmacological identification of the major signal transduction pathways involved in Aqp8bb mitochondrial trafficking in seabream spermatozoa. (*A*) Dose–response inhibition of the percentage of activated spermatozoa showing Aqp8bb and MTR mitochondrial colocalization after treatment with DMSO alone (vehicle) or containing different protein kinase inhibitors determined by immunofluorescence microscopy. (*B*) Representative Aqp8bb immunoblots in mitochondrial extracts (*Upper*), and corresponding quantitation normalized to Phb (*Lower*), from sperm in *A* treated with 10 μM of the different drugs. (*C*) Total and phosphorylated JNK and GSK3 representative immunoblots (*Upper*) in sperm from *B*, and densitometric analysis of kinase phosphorylation normalized to the corresponding total kinase blot (*Lower*). (*D* and *E*) Activation of mitochondrial Aqp8bb trafficking in immotile spermatozoa maintained in NAM and exposed to activators of JNK (ANS), PKC (PMA), or GSK3 (MK2206) (black color) determined by immunofluorescence microscopy (*D*) and immunoblotting (*E*). Inhibition of ANS (10 μM)-induced Aqp8bb transport by inhibitors of GSK3 (CHIR99021) and PKC (BIM-II) is shown in red color. (*F*) MKK4, JNK, and GSK3 activation in sperm treated as in *D*. (*G*) Proposed model of the JNK and GSK3 signaling pathways controlling Aqp8bb mitochondrial transport in activated seabream spermatozoa. The kinase inhibitors (red color) and activators (green color) used are indicated. In *A*–*F*, data (mean ± SEM; $n = 3$ to 7 fish) were statistically analyzed by one-way ANOVA (*P* values for each compound are indicated in *A* and *D*). ***$P < 0.001$; **$P < 0.01$; *$P < 0.05$, with respect to control spermatozoa (treated with DMSO vehicle) or as indicated in brackets, or with respect to sperm treated with ANS alone (*E* and *F* in parenthesis).

cascade can partially activate GSK3, and that PKC activity is required for full JNK and GSK3 activation. This combination can explain the somewhat lower potency of PKC inhibition to prevent Aqp8bb mitochondrial transport. However, the strong reduction of Aqp8bb trafficking by JNK inhibition suggests an additional role of JNK on channel trafficking that is not mediated by GSK3.

In order to assess the potential interaction of the JNK, PKC, and GSK3 pathways in the regulation of Aqp8bb mitochondrial transport, we investigated whether this mechanism could be stimulated in immotile spermatozoa. For this, NAM-maintained sperm were treated with the JNK/p38 MAPK phosphorylation-inducer anisomycin (ANS) and the PKC analog activator phorbol 12-myristate 13-acetate (PMA), as well as with MK2206 and SH-5, which are AKT/PKB inhibitors that can indirectly activate GSK3 (39, 40). The data show that all of these drugs stimulated Aqp8bb mitochondrial trafficking, while treatment with the PKC inactive enantiomer 4α-PMA had no effect (Fig. 2 *D* and *E* and *SI Appendix*, Fig. S4*A*). However, the percentage of spermatozoa showing Aqp8bb localization in the mitochondrion after exposure to ANS was similar to that observed in SW-activated sperm, whereas the other compounds only promoted channel mitochondrial accumulation in approximately half of the cells (Fig. 2 *D* and *E* and *SI Appendix*, Fig. S4*A*). The stimulatory effect of ANS on Aqp8bb trafficking, which occurs through JNK and not p38 MAPK (*SI Appendix*, Fig. S4 *B* and *C*), was completely blocked by GSK3 inhibition, but only partially reduced by the PKC inhibitors BIM-II and calphostin C (Fig. 2 *D* and *E* and *SI Appendix*, Fig. S4*A*). This suggests that PKC activation by JNK is necessary to drive Aqp8bb mitochondrial transport, but that this mechanism can still be triggered to some extent by JNK independently of PKC. The positive effects of PMA and MK2206 on Aqp8bb transport were not additive and could be reduced by JNK and GSK3 inhibition (*SI Appendix*, Fig. S4 *D* and *E*), suggesting that PKC and GSK3 activate the same mechanism for Aqp8bb trafficking, with both kinases dependent on active JNK.

Activation of JNK and PKC by ANS and PMA treatments, respectively, in immotile spermatozoa induced the phosphorylation of JNK$^{T183/Y185}$ and GSK3α/β$^{Y279/216}$, thus supporting that JNK and GSK3 can be activated via PKC, and that activation of GSK3 by JNK occurs during Aqp8bb trafficking (Fig. 2*F*). In contrast, MK2206 activated GSK3 but not JNK, indicating that GSK3 is downstream of JNK (Fig. 2*F*). However, as noted earlier, active JNK was still necessary for MK2206-induced Aqp8bb transport, thus supporting a role of JNK regulating mitochondrial

Aqp8bb transport independently of GSK3. The ANS-mediated $JNK^{T183/Y185}$ phoshorylation was not affected by PKC or GSK3 inhibition, while that of GSK3α/$β^{Y279/216}$ was moderately reduced by PKC inhibition but it was not affected by the GSK3 blocker (Fig. 2*F*). Therefore, this also confirms that JNK can partially activate GSK3 in the absence of PKC activation.

Taken together, our findings suggest that a cross-talk between the PKC and JNK signaling pathways triggers the GSK3-mediated trafficking of the Aqp8bb peroxiporin to the inner mitochondrial membrane of the seabream spermatozoon (Fig. 2*G*). Moreover, a direct additive action of JNK, which bypasses the GSK3 pathway, acts as a multiplier for the rapid trafficking mechanism (Fig. 2*G*).

GSK3 and JNK Control Aqp8bb-Mediated Mitochondrial Detoxification in Activated Seabream Spermatozoa. Since JNK and GSK3 appear to be key regulators of Aqp8bb trafficking, we investigated whether the pharmacological blockage of their activities can impair Aqp8bb insertion into the spermatozoon inner mitochondrial membrane and hamper H_2O_2 efflux. An Aqp8bb immunoblot of inner membrane mitochondrial extracts from SW-activated spermatozoa confirmed that the amount of mitochondrial Aqp8bb was lower in sperm treated with the JNK and GSK3 inhibitors compared to controls (Fig. 3*A*). The low mitochondrial abundance of Aqp8bb in these groups was associated with a reduced ability of mitochondria to transport H_2O_2 as measured with the ROS-sensitive, cell permeable fluorescent dye 5-(and -6)-chloromethyl-2′,7′-dichlorodihydrofluorescein diacetate, acetyl ester (CM-H_2DCFDA) (Fig. 3*B*). As a consequence, a higher accumulation of H_2O_2 in the spermatozoa exposed to the JNK and GSK3 inhibitors with respect to controls was observed during activation (Fig. 3*C*). The increased intracellular ROS was harmful to sperm function since time-course monitoring of sperm motion kinetics using computer-assisted sperm analysis (CASA) for up to 180 s revealed that both inhibitors reduced the percentage of motility and progressivity of the spermatozoa, as well as their curvilinear velocity (VCL), with respect to sperm treated with DMSO alone (Fig. 3*D*). However, the three sperm motion parameters measured within the first 30 s postactivation were more diminished when the JNK pathway is blocked (17 ± 1% and 35 ± 5% inhibition with the GSK3 and JNK blockers, respectively, with respect to the controls; $n = 9$, $P = 0.003$, Student's t test). The addition of the mitochondria-targeted antioxidant Mito-TEMPO recovered sperm motion kinetics within 60 to 70 s, except there was reduction in the percentage of motile spermatozoa induced by GSK inhibition (Fig. 3*E*). This suggests that GSK3 likely plays other roles to maintain sperm motility in addition to mitochondrial Aqp8bb trafficking. These observations are thus consistent with a role of the JNK and GSK3 signaling pathways regulating Aqp8bb mitochondrial detoxification and the kinematic properties of the spermatozoa.

Intracellular Ca^{2+} and ROS Trigger Seabream Aqp8bb Mitochondrial Transport. We previously demonstrated that prevention of the intracellular Ca^{2+} surge that normally occurs in seabream sperm upon SW activation partially inhibits mitochondrial Aqp8bb trafficking (41), and that the SW-induced hyperosmotic shock increases ROS levels in the spermatozoa (26). Since it is known that the ASK1-MAPK signaling pathway can be activated by cellular oxidative stress (42), we hypothesize that elevated intracellular concentrations of Ca^{2+} ($[Ca^{2+}]_i$) and ROS linked to the hyperosmotic shock in SW are the upstream signals in seabream spermatozoa triggering JNK and GSK3 activation and Aqp8bb intracellular trafficking.

To investigate this hypothesis, we first determined the contribution of Ca^{2+}-activated signaling pathways in the regulation of Aqp8bb mitochondrial transport by treating immotile sperm with 3 mM Ca^{2+} in the presence of 10 μM of the Ca^{2+} ionophore A23187, which generates similar levels of $[Ca^{2+}]_i$ to those determined in SW-activated sperm (Fig. 4*A*). Under these conditions, Aqp8bb transport to the mitochondria was enhanced, but interestingly, the percentage of spermatozoa showing mitochondrial localization of the channel was approximately half of that observed in SW-activated sperm (Fig. 4*B*). Ca^{2+}-triggered Aqp8bb trafficking was not affected by inhibitors of ASK1 and MKK, whereas it was reduced to control levels by blockers of PKC, JNK, and GSK3 (Fig. 4*C* and *SI Appendix*, Fig. S5). After Ca^{2+} treatment, the inhibitory phosphorylation of $ASK1^{S966}$ did not change, and MKK4 was not activated, while phosphorylation of $JNK^{T183/Y185}$ and GSK3α/$β^{Y279/216}$ was enhanced (Fig. 4*D*). The activation of JNK and GSK3 was reduced by PKC inhibition, while the blockage of JNK only partially diminished GSK3 activation (Fig. 4*D*). These data suggest that a $[Ca^{2+}]_i$ surge alone can partially trigger JNK- and GSK3-mediated Aqp8bb mitochondrial transport through PKC activation of JNK and GSK3, and thus independently of the ASK1-MKK4 signaling pathway.

To examine the effect of oxidative stress on Aqp8bb intracellular trafficking in spermatozoa, independently of the Ca^{2+} signal, we followed two different approaches: The generation of ROS in immotile sperm by exposure to the xanthine-xanthine oxidase (X-XO) system (43), and the treatment of SW-activated sperm with the Ca^{2+} chelator 1,2-bis(2-aminophenoxy)ethane-N,N,N′,N′-tetraacetic acid (BAPTA) in the presence or absence of diphenyleneiodonium (DPI), a compound that limits ROS production by inhibiting membrane-bound NADPH oxidases (NOXes) and other flavoproteins (44). External treatment of nonactivated sperm with X-XO produced an increment of ROS in a dose–response manner, the highest X-XO dose generating similar ROS levels to those measured in SW-activated sperm (Fig. 5 *A* and *D*). Upon SW activation, treatment with BAPTA abolished the $[Ca^{2+}]_i$ surge in a dose-dependent manner, which completely inhibited motility (*SI Appendix*, Fig. S6*A*), while ROS accumulation in the spermatozoa was not affected (Fig. 5 *B* and *D*). Conversely, exposure of activated sperm to DPI decreased ROS levels but did not affect the increase of $[Ca^{2+}]_i$ (Fig. 5 *C* and *D*). Interestingly, as previously observed in Ca^{2+}-treated immotile sperm, treatment of immotile spermatozoa with the highest dose of X-XO stimulated Aqp8bb mitochondrial trafficking in approximately half of the spermatozoa with respect to SW-activated sperm exposed to DMSO alone (*SI Appendix*, Fig. S6*B*). The same result was observed in sperm activated in SW containing BAPTA (*SI Appendix*, Fig. S6*C*).

In both ROS- and SW+BAPTA-treated spermatozoa, Aqp8bb mitochondrial accumulation was completely inhibited by blockers of ASK1, MKK, JNK, and GSK3, whereas inhibition of PKC only partially decreased Aqp8bb transport (Fig. 5*E* and *SI Appendix*, Fig. S6 *B–D*). The ROS generated in immotile and SW spermatozoa activated ASK1 by deposphosphorylation of the inhibitory $ASK1^{S966}$ site, which was not affected by any of the downstream kinase inhibitors, while it enhanced the phosphorylation of $MKK4^{T261}$, $JNK^{T183/Y185}$, and GSK3α/$β^{Y279/216}$ (Fig. 5*F* and *SI Appendix*, Fig. S6*E*). Activation of MKK4 was reduced to control levels by inhibitors of ASK1 and MKK, but not by inhibition of downstream kinases, whereas ROS-induced JNK and GSK3 activation was completely blocked by ASK1 and MKK inhibitors, and only partially prevented by PKC inhibition (Fig. 5*F* and *SI Appendix*, Fig. S6*E*). However, JNK inhibition strongly reduced ROS-mediated GSK3 activation (Fig. 5*F* and *SI Appendix*, Fig. S6*E*), which indicates that the ROS-triggered ASK1-MKK4-JNK pathway can activate GSK3 independently of PKC. The data, however, also suggest that ROS-induced PKC activity may be a positive regulator of JNK, as previously observed after Ca^{2+} treatment alone, but that in this case this mechanism requires previous activation of JNK by the canonical upstream kinase MKK4.

Consistent with this model, when either the $[Ca^{2+}]_i$ or ROS increments in SW-activated sperm were completely abolished by BAPTA and DPI, respectively, the percentage of spermatozoa showing mitochondrial localization was similar to that elicited by

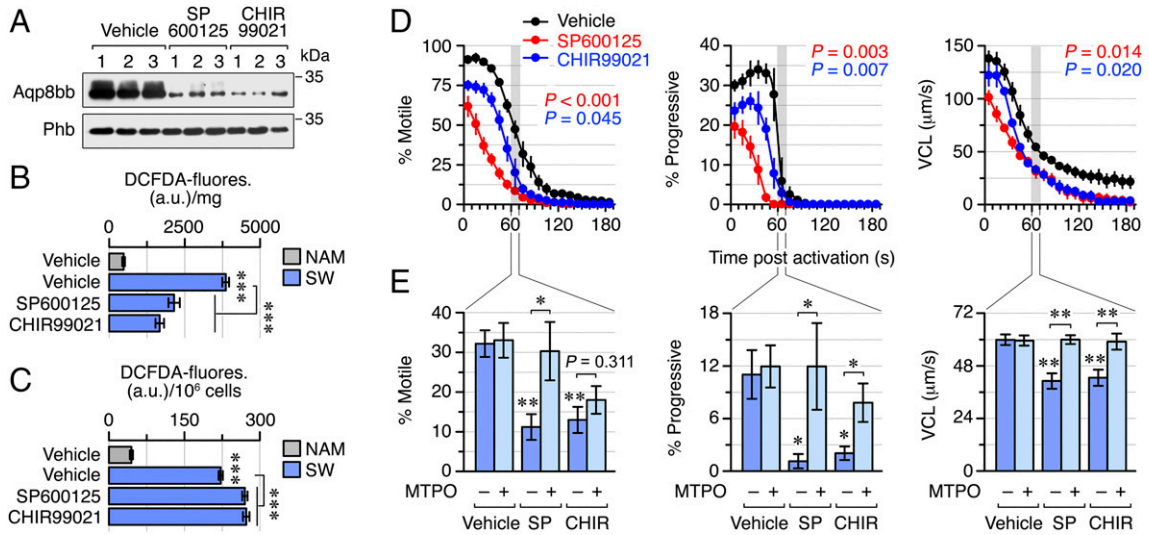

Fig. 3. JNK and GSK3 inhibition prevents Aqp8bb insertion into the seabream spermatozoa inner mitochondrial membrane upon SW activation. (*A*) Aqp8bb immunoblot in the inner mitochondrial membrane from SW-activated spermatozoa ($n = 3$ fish) exposed or not to 10 μM of the JNK (SP600125) and GSK3 (CHIR99021) inhibitors. Phb was used as a marker for even loading. (*B*) H_2O_2 uptake (mean ± SEM, $n = 6$ fish) by mitochondria isolated from NAM and SW spermatozoa treated with or without the inhibitors. (*C*) ROS levels (mean ± SEM, $n = 8$ fish) in spermatozoa treated as in *B*. Statistical differences were measured by one-way ANOVA. ***$P < 0.001$, with respect to NAM or SW-activated sperm not treated with the inhibitors, or as indicated in brackets. (*D*) Percentage of motility and progressivity, and VCL, of spermatozoa (mean ± SEM, $n = 4$ fish) treated with DMSO in the presence or absence of SP600125 and CHIR99021. Statistical differences with respect to control spermatozoa (only during the first 60 s for motility and progressivity) were determined by the Mann–Whitney *U* test (*P* values indicated in each panel). (*E*) Effect of the mitochondria-targeted antioxidant Mito-TEMPO (MTPO; 50 μM) on the SP600125 (SP) or CHIR99021 (CHIR) inhibition of sperm kinetics (mean ± SEM, $n = 7$ fish) at 60 to 70 s postactivation (marked with a gray bar in *D*). Data are statistically analyzed by one-way ANOVA (minus MTPO), and by the unpaired Student's *t* test between sperm untreated and treated with MTPO. *$P < 0.05$; **$P < 0.01$; ***$P < 0.001$, with respect to nontreated sperm, or as indicated in brackets.

ROS treatment of immotile spermatozoa, and was approximately half of that observed in SW-activated sperm (Fig. 5 *G* and *H*). However, when both inhibitors were present upon SW activation, Aqp8bb mitochondrial accumulation was strongly reduced to the level observed in immotile spermatozoa (Fig. 5 *G* and *H*). Kinase phosphorylation analysis showed that while ASK1 activation in SW-activated spermatozoa was not affected by BAPTA treatment, DPI reduced both ASK1 and MKK4 activation (Fig. 5*I*). In contrast, each of the BAPTA and DPI treatments only partially prevented JNK and GSK3 activation (Fig. 5*I*). In the presence of BAPTA plus DPI, the activation state of ASK1 and MKK4 did not change with respect to that observed in the presence of DPI alone, whereas the activation of JNK and GSK3 was strongly diminished (Fig. 5*I*).

Taken together, these findings suggest that the intracellular Ca^{2+} and ROS signals occurring in SW-activated seabream spermatozoa respectively trigger alternative and additive PKC and ASK1-MAPK pathways, which cross-talk to activate JNK and GSK3 and direct Aqp8bb mitochondrial insertion.

JNK and GSK3 Can Phosphorylate Seabream Aqp8bb In Vitro. In silico analysis of the seabream Aqp8bb amino acid sequence revealed the presence of three Ser residues (Ser^{16}, Ser^{19}, and Ser^{20}) and one Thr (Thr^{24}) residue in the N terminus of the channel as potential phosphorylation recognition sites for GSK3 and proline-directed kinase (such as p38 MAPK and JNK), respectively (*SI Appendix*, Fig. S7*A*). An additional Ser residue (Ser^{91}) showing a low score for GSK3 and proline-directed kinase phosphorylation was also identified in the first cytoplasmic loop (*SI Appendix*, Fig. S7*A*). To experimentally assess whether GSK3 and JNK can phosphorylate seabream Aqp8bb, we employed in vitro phosphorylation assays using mouse recombinant JNK1 (rJNK1) and human recombinant GSK3β (rGSK3). In these experiments, Flag-tagged Aqp8bb (Aqp8bb-Flag) transiently expressed in embryonic kidney cells 293T (HEK293T) was immunoprecipitated using the seabream Aqp8bb specific antibody and incubated with rJNK1 or rGSK3β in the presence or absence of ATP. Immunobloting of immunoprecipitated Aqp8bb-Flag using phosphorylated Ser- and Thr-specific antibodies confirmed the ATP-dependent specific phosphorylation of Aqp8bb Ser and Thr residues by rJNK1, and only of Ser residues by rGSK3β (*SI Appendix*, Fig. S7*B*). To determine which specific channel residues are phosphorylated by the kinases, the same assays were carried out using wild-type Aqp8bb-Flag (Aqp8bb-Flag-WT) or Aqp8bb-Flag constructs in which all Ser and Thr residues in the N terminus, as well as Ser^{91}, were independently mutated into Ala. The results showed that Aqp8bb-Flag-T24A and -S91A prevented rJNK1 Thr and Ser phosphorylation, respectively, whereas Aqp8bb-Flag-S16A abolished Ser phosphorylation by rGSK3β (*SI Appendix*, Fig. S7*C*). These data therefore indicate that Thr^{24} and Ser^{91} are the residues phosphorylated by rJNK1, while only Ser^{16} is the target site for rGSK3β.

The majority of GSK3 substrates require prephosphorylation at a residue 4 or 5 amino acids C-terminal to the GSK3 target site for full catalytic activity, a phenomenon referred to as "priming" (45). The seabream Aqp8bb shows two such potential priming sites, Ser^{19} and Ser^{20}, located three and four residues C-terminal to the Ser^{16} GSK3 phosphorylation site (*SI Appendix*, Fig. S7*A*). In addition, Thr^{24} could also play a role since some substrates of GSK3 show a priming site much further from the target site (45). To investigate whether a priming mechanism regulates rGSK3β-mediated Aqp8bb phosphorylation at Ser^{16}, we first established by immunoblotting the lowest amount of rGSK3β to yield detectable levels of Ser phosphorylation in Aqp8bb (*SI Appendix*, Fig. S7*D*), and subsequently test if Aqp8bb-Flag-S19D, -S20D, and -T24D mutants, which mimic a phosphorylated state, increase rGSK3β-mediated channel phosphorylation. The results show that Ser^{16} phosphorylation of Aqp8bb-Flag by rGSK3β was increased by ~27 times in Aqp8bb-Flag-S19D and -S20D mutants with respect to the wild-type, whereas the Aqp8bb-Flag-T24D was phosphorylated

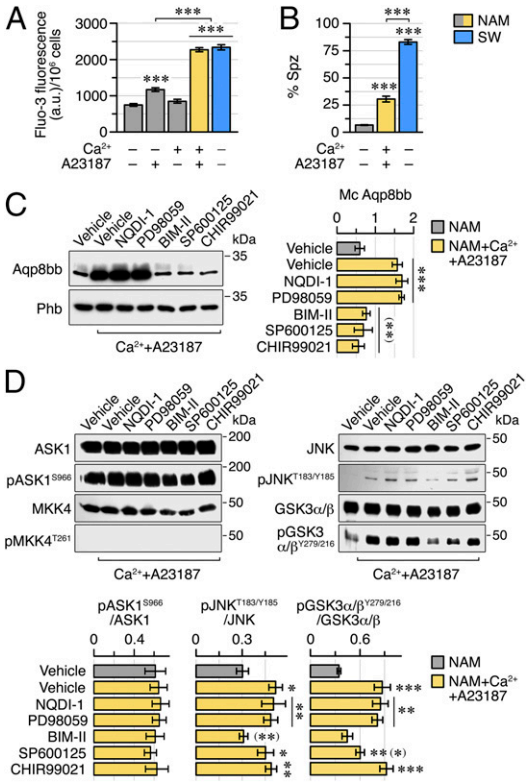

Fig. 4. An intracellular Ca^{2+} surge partially drives Aqp8bb transport to the mitochondrion in nonactivated seabream spermatozoa. (*A*) Intracellular Ca^{2+} levels in sperm maintained in NAM and treated with 3 mM Ca^{2+} and/or 10 μM of the Ca^{2+} ionophore A23187, and in SW-activated sperm. (*B*) Percentage of spermatozoa showing Aqp8bb mitochondrial localization after exposure to Ca^{2+} and A23187 in NAM, or upon activation in SW. (*C*) Representative immunoblot of mitochondrial Aqp8bb (*Left*), and corresponding quantitation normalized to Phb (*Right*), from sperm incubated with or without Ca^{2+} and A23187 in NAM, and treated with 10 μM of different kinase inhibitors. (*D*) Total and phosphorylated ASK1, MKK4, JNK, and GSK3α/β representative immunoblots (*Upper*) in spermatozoa treated as in *C*. (*Lower*) Depiction of the densitometric analysis of kinase phosphorylation normalized to the corresponding band from the total kinase blot. Data are the mean ± SEM (n = 4 to 6 fish) and are statistically analyzed by one-way ANOVA. ***$P < 0.001$; **$P < 0.01$; *$P < 0.05$, with respect to nontreated sperm, or treated with Ca^{2+}+A23187 without inhibitors (in parenthesis), or as indicated in brackets.

at Ser^{16} ~12 times more efficiently (*SI Appendix*, Fig. S7*E*). These findings therefore suggest that Aqp8bb phosphorylation of Ser^{19}, Ser^{20}, and to a lesser extent Thr^{24}, can prime the channel N terminus for Ser^{16} phosphorylation by GSK3 (*SI Appendix*, Fig. S7*F*).

GSK3 and JNK Phosphorylation of Ser^{16} and Thr^{24}, Respectively, in Seabream Aqp8bb Regulate Channel Trafficking. Transcriptional and translational activity in ejaculated sperm is very low or completely absent (46). Therefore, in order to investigate the molecular basis of Aqp8bb mitochondrial trafficking, we examined whether the signaling pathways controlling this mechanism in spermatozoa can be reproduced in cultured mammalian cells. For these tests, we selected the human hepatocarcinoma-derived cell line HepG2 in which the AQP8 ortholog is expressed in the inner mitochondrial membrane (47). The results of these experiments showed that the same Ca^{2+}-activated PKC-GSK3 and H_2O_2-activated JNK-GSK3 signaling cascades controlling Aqp8bb mitochondrial transport in the seabream spermatozoon can be replicated in HepG2 cells, except that in this case the cross-talk between PKC and JNK does not occur (*SI Appendix*, *Supplementary Text S1* and Fig. S8).

Using the HepG2 cells as a surrogate system for functional analyses, we investigated the role of Aqp8bb phosphorylation on mitochondrial channel trafficking. To this end, we transfected cells with Aqp8bb-Flag-WT or single phosphomimetic mutants at each Ser and Thr residue in the N terminus of the channel (Aqp8bb-Flag-T2D, -T15D, -S16D, -S19D, -S20D, -T24D), and at Ser^{91} (Aqp8bb-Flag-S91D), or with a S16D/T24D double mutant, and subsequently determined mitochondrial targeting of the encoded proteins by immunofluorescence microscopy. The data showed that Aqp8bb-Flag-WT and the Aqp8bb-Flag-S91D mutant mainly remained in the cell plasma membrane, whereas the Aqp8bb-Flag-T2D and -T15D channels were retained in the cytoplasm (Fig. 6*A* and *SI Appendix*, Fig. S9*A*). In contrast, the Aqp8bb-Flag-S19D and -S20D mutants were partially targeted to the mitochondria, which appears to be enhanced for the Aqp8bb-Flag-S16D, -T24D and S16D/T24D channel constructs (Fig. 6*A*). Immunoblot analysis showed that the wild-type and mutant channels were expressed at similar levels, and confirmed that each of the Aqp8bb-Flag-S16D and -T24D mutants were targeted to the mitochondria, unlike the Aqp8bb-Flag-WT (Fig. 6*B*). The Aqp8bb-Flag-S19D and -S20D constructs also accumulated in the mitochondria but to a lesser amount than the Aqp8bb-Flag-S16D and -T24D mutants (Fig. 6*B*). However, the data also revealed that the Aqp8bb-Flag-S16D/T24D double mutant was more concentrated in the mitochondria than each of the corresponding single mutants (Fig. 6*B*), suggesting that phosphorylation of Ser^{16} and Thr^{24} residues in the channel are additive for activating mitochondrial transport.

To further investigate the role of Ser^{16} and Thr^{24} phosphorylation driving Aqp8bb mitochondrial trafficking, cells were transfected with Aqp8bb-Flag-WT or mutant channels in which one or both Ser^{16} and Thr^{24} were mutated into Cys or Ala, respectively, and treated with 10 mM Ca^{2+} and 100 μM H_2O_2. Immunoblot analyses of total protein extracts showed that the three Aqp8bb-Flag-S16C, -T24A, and -S16C/T24A mutants were equally expressed than the Aqp8bb-Flag-WT (*SI Appendix*, Fig. S9*B*). However, mitochondrial trafficking in response to Ca^{2+} and H_2O_2 treatment was similarly reduced in both Aqp8bb-Flag-S16C and -T24A constructs with respect to that shown by the Aqp8bb-Flag-WT, whereas channel transport of the Aqp8bb-Flag-S16C/T24A double mutant was almost completely abolished (Fig. 6*C*). Immunoprecipitation followed by immunoblot analysis of phosphorylated Ser and Thr showed that Aqp8bb-Flag-WT was phosphorylated at Ser and Thr residues in response to Ca^{2+} and H_2O_2 uptake (Fig. 6*C*). However, only Ser or Thr phosphorylation was reduced in the Aqp8bb-Flag-S16C and -T24A constructs, respectively, with respect to that seen in the Aqp8bb-Flag-WT, while phosphorylation of both Ser and Thr residues was decreased in the Aqp8bb-Flag-S16C/T24A double mutant (Fig. 6*C*). These data therefore support that Ser^{16} and Thr^{24} phosphorylation in the Aqp8bb N terminus are both necessary for maximum mitochondrial channel transport.

To confirm that GSK3 and JNK are, respectively, involved in Ser^{16} and Thr^{24} phosphorylation of Aqp8bb, HepG2 cells were cotransfected with Aqp8bb-Flag-WT and dominant-negative catalytically inactive forms of *Xenopus laevis* GSK3β (dnGSK3β) (48) or human JNK1 (dnJNK1) (49), and exposed to external Ca^{+2} and H_2O_2. Both inhibitory constructs reduced the accumulation of Aqp8bb-Flag-WT in the mitochondria in response to external Ca^{2+} and ROS (Fig. 6*D*), thus further supporting the role of JNK and GSK3 in the Aqp8bb trafficking mechanism. However, while dnGSK3β expression decreased Ser phosphorylation of Aqp8bb-Flag-WT, but not Thr phosphorylation, the dnJNK1 construct completely abolished Ser and Thr phosphorylation of the channel (Fig. 6*D*). These findings suggest that JNK could activate GSK3 for Aqp8bb Ser phosphorylation, in addition to its potential role

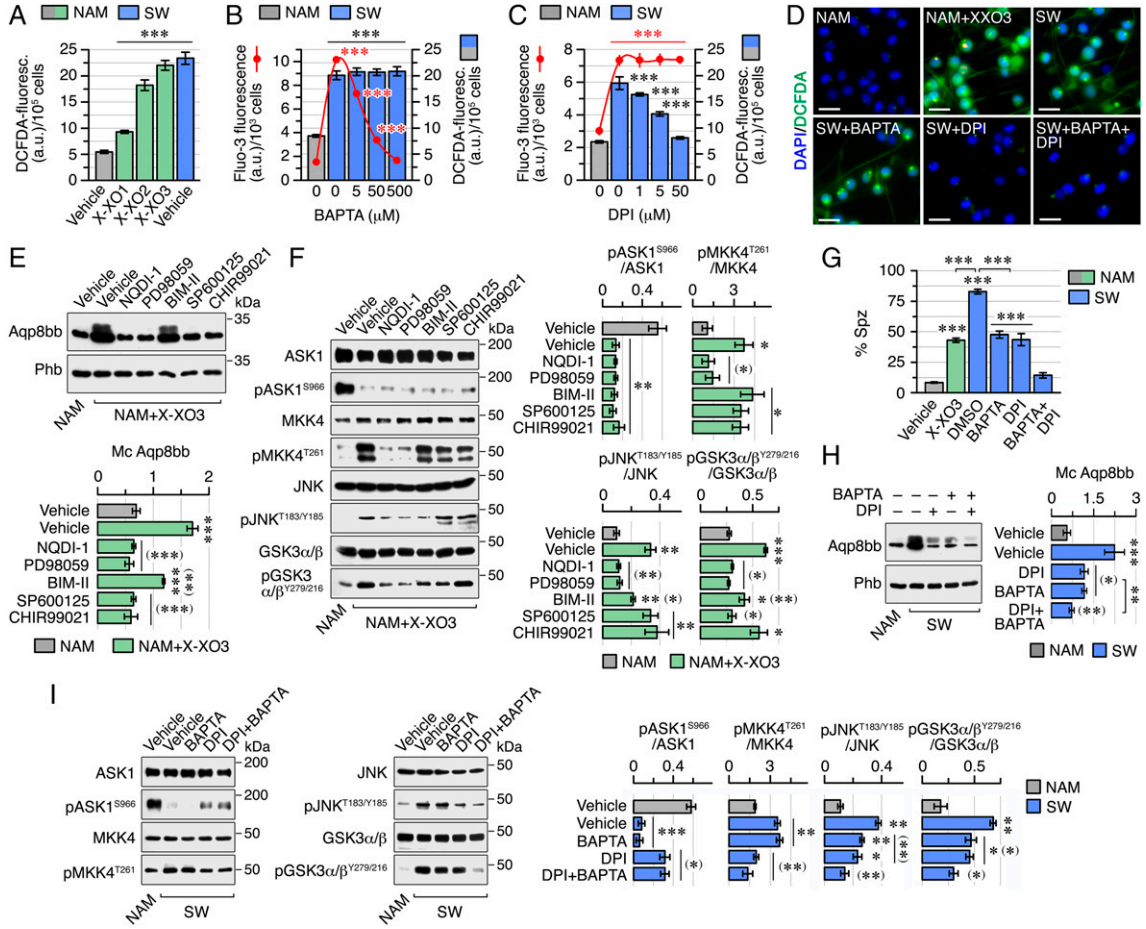

Fig. 5. Oxidative stress-induced Aqp8bb mitochondrial transport in seabream spermatozoa. (*A*) ROS levels in immotile sperm treated with increasing doses of X-XO (X-XO1, X-XO2, and X-XO3), and in SW-activated spermatozoa. (*B* and *C*) Intracellular Ca^{2+} (red line) and ROS levels (bars) in nonactivated and activated sperm in the presence of BAPTA (*B*) or DPI (*C*). (*D*) Epifluorescence photomicrographs of nonactivated and activated spermatozoa treated with X-XO3, 500 μM BAPTA, 50 μM DPI, or BAPTA+DPI, and labeled with the CM-H_2DCFDA dye (green). Nuclei are counterstained with DAPI (blue). (Scale bars, 5 μm.) (*E*) Immunoblot of mitochondrial Aqp8bb in sperm maintained in NAM and exposed to X-XO3 (*Upper*), in the presence or absence of 10 μM of kinase inhibitors, and corresponding quantitation normalized to Phb (*Lower*). (*F*) Total and phosphorylated ASK1, MKK4, JNK, and GSK3α/β immunoblots (*Left*), and densitometric analysis of phosphorylated forms normalized to the corresponding nonphosphorylated bands (*Right*), in spermatozoa treated as in *E*. (*G*) Percentage of spermatozoa showing Aqp8bb in mitochondria after treatment with X-XO3 in NAM, or upon activation in SW with or without BAPTA and/or DPI. (*H*) Immunoblot of mitochondrial Aqp8bb in immotile sperm or activated in SW with or without BAPTA and/or DPI (*Left*) and quantitation normalized to Phb (*Right*). (*I*) Immunoblots of kinase activation in sperm treated as in *H* (*Left*) and quantitation of phosphorylated forms. In all panels, data are displayed as mean ± SEM ($n = 4$ to 6 fish) and are statistically analyzed by one-way ANOVA. ***$P < 0.001$; **$P < 0.01$; *$P < 0.05$, with respect to nontreated spermatozoa in NAM, spermatozoa exposed to NAM plus X-XO3 or SW without inhibitors (in parenthesis), or as indicated in brackets (*G* and *E*).

phosphorylating Thr^{24} in the channel, as previously predicted to occur in sperm cells. To corroborate this hypothesis, activation of GSK3 was evaluated in HepG2 cells expressing Aqp8bb-Flag-WT and dnJNK1 and treated with Ca^{2+} and H_2O_2. The data confirmed that phosphorylation of GSK3α/$\beta^{Y279/216}$ was reduced in the presence of catalytically inactive JNK1, whereas that of GSK3α^{S21}, but not of GSK3β^{S9}, was increased (Fig. 6*E*). These results therefore suggest that mitochondrial trafficking of seabream Aqp8bb is regulated by Ser^{16} phosphorylation by JNK- and PKC-activated GSK3, as well as by JNK-mediated Thr^{24} phosphorylation of the channel.

Aqp8bb Mitochondrial Transport in FW Spermatozoa Is Controlled by PKC or GSK3 Phosphorylation of an N-Terminal Ser Residue. To examine whether the same signaling pathways regulating seabream Aqp8bb mitochondrial transport are present in FW spermatozoa, we initially assessed the effect of PKC, JNK, and GSK3 inhibitors (BIM-II, SP600125, and CHIR99021, respectively) on Aqp8bb trafficking in Atlantic salmon and zebrafish spermatozoa upon FW activation. In contrast to the seabream, the results showed that JNK inhibition did not affect mitochondrial channel transport in salmon and zebrafish sperm, indicating that the JNK signaling pathway is not involved in this mechanism (Fig. 7*A*). In contrast, both PKC and GSK3 inhibitors reduced the percentage of salmon spermatozoa showing Aqp8bb mitochondrial localization in a dose–response manner, whereas only the blockage of PKC elicited the same effect in zebrafish (Fig. 7*A*). These observations suggest a role of PKC and GSK3, and of PKC only, in the control of Aqp8bb transport in salmon and zebrafish spermatozoa, respectively.

To confirm that PKC is the signaling kinase controlling Aqp8bb-mediated mitochondrial detoxification in zebrafish spermatozoa, the levels of ROS in immotile and FW-activated sperm in the presence or absence of the PKC inhibitor BIM-II were determined. The results showed that the hypoosmotic shock in FW does not increase ROS levels in zebrafish sperm; however, when the transport of Aqp8bb to the mitochondria was impaired by PKC inhibition, ROS levels were increased (Fig. 7*B*). This reveals that an osmotic shock-induced ROS-MAPK-JNK signaling pathway

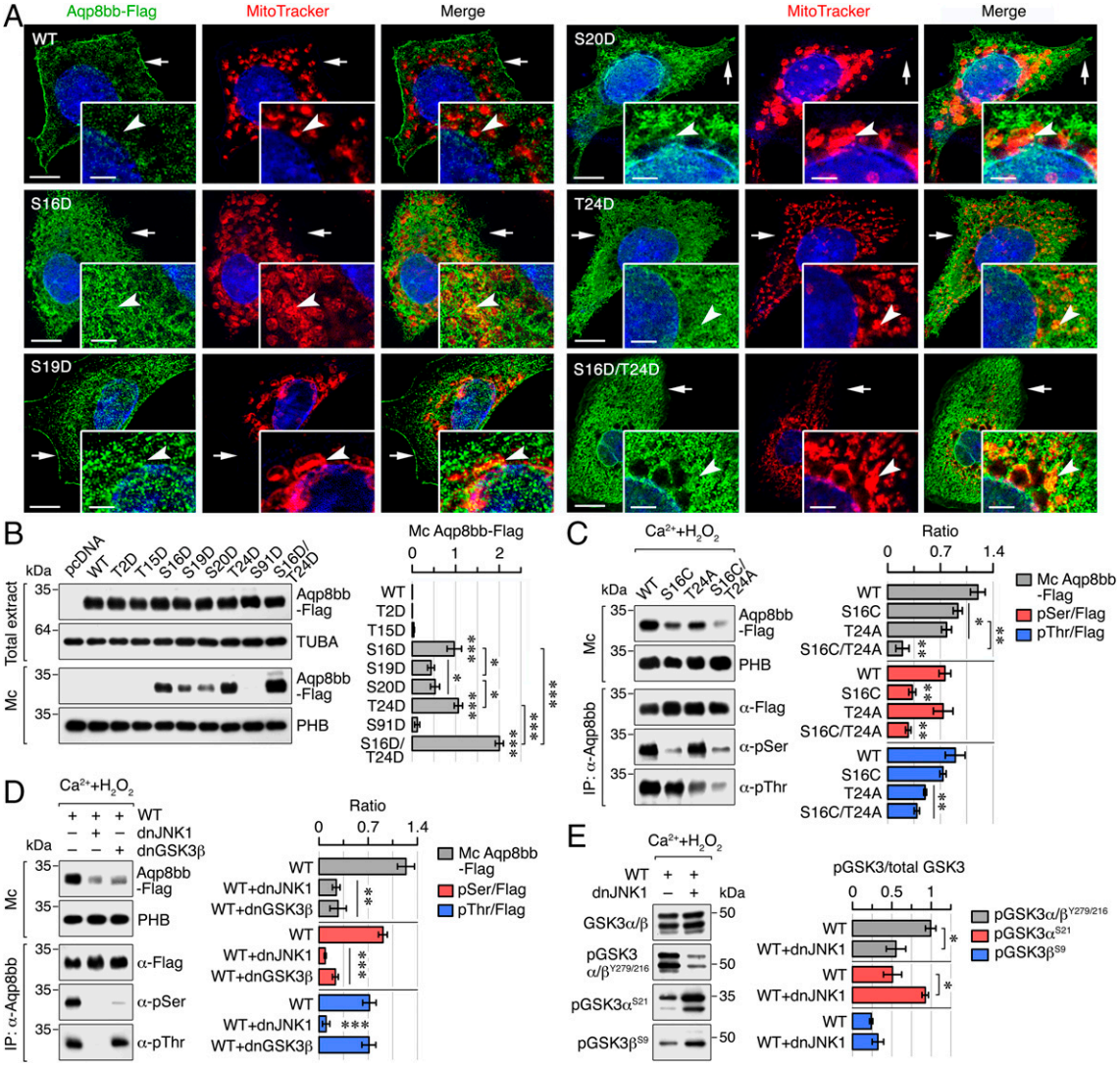

Fig. 6. Dual N terminus phosphorylation of seabream Aqp8bb by GSK3 and JNK control mitochondrial channel transport in HepG2 cells. (*A*) Double staining of Aqp8bb-Flag (green) and mitochondria (MTR, red) in cells transiently expressing wild-type Aqp8bb-Flag (WT) or phospho-mimetic mutants as indicated. Arrows point to the plasma membrane, whereas arrowheads indicate colocalized signals in the mitochondria. (Scale bars, 10 μm; *Insets*, 5 μm.) (*B*) Representative immunoblot of total and mitochondrial Aqp8bb-Flag-WT and mutants, using tubulin (TUBA) and PHB as loading controls, respectively (*Left*). Mitochondrial Aqp8bb-Flag quantitation is normalized to PHB (*Right*). (*C*) Immunoblot of mitochondrial Aqp8bb-Flag-WT and -S16C, -T24A, and -S16C/T24A mutant channels, and Ser and Thr phosphorylation of the corresponding immunoprecipitated proteins, in cells treated with Ca^{2+} and H_2O_2. (*Right*) The amount of each construct in the the mitochondria, normalized to PHB, and their Ser and Thr phosphorylation state normalized to the total immunoprecipitated protein. (*D*) Effect of coexpression of Aqp8bb-Flag-WT and dominant-negative forms of JNK1 and GSK3β (dnJNK1 and dnGSK3β, respectively) on the mitochondrial transport and Ser/Thr phosphorylation of the channel in cells treated as in *C*. (*E*) Immunoblot of nonactivated and activated GSK3 in cells coexpressing Aqp8bb-Flag-WT and dnJNK1 and treated with Ca^{2+} and H_2O_2 (*Left*), and densitometric analysis of phosphorylated GSK3 forms (*Right*). In *B* and *C*, quantifications are displayed as mean ± SEM ($n = 3$ separate experiments), and data are statistically analyzed by one-way ANOVA (*B–D*) or by an unpaired Student's *t* test (*E*). ***$P < 0.001$; **$P < 0.01$; *$P < 0.05$, with respect Aqp8bb-Flag-WT or as indicated in brackets.

controlling Aqp8bb trafficking is absent in zebrafish spermatozoa. As observed for seabream sperm, high levels of intracellular ROS induced by PKC inhibition also reduced the percentage of motility and progressivity and the VCL of zebrafish spermatozoa (Fig. 7*C*). However, in this case Mito-TEMPO treatment only partially recovered the kinematic properties (Fig. 7*D*), suggesting that PKC plays an additional role for sperm motility and velocity maintenance in zebrafish that is unrelated to the mitochondrial peroxiporin transport mechanism.

Comparison of the deduced amino acid sequences of the Aqp8bb N terminus from seabream, salmon, and zebrafish revealed a Ser residue in position 14 or 16 in all three species, whereas the JNK Thr^{24} phosphorylation site from seabream Aqp8bb was missing in the two FW spawning teleosts. In silico analysis revealed that Ser^{14} from salmon Aqp8bb is a putative phosphorylation site for GSK3, as is Ser^{16} from seabream Aqp8bb, including a potential priming site at Ser^{18}, whereas Ser^{16} in zebrafish Aqp8bb is a presumed residue for PKC phosphorylation (Fig. 7*E*). To confirm that these target sites in salmon and zebrafish Aqp8bb are functional, in vitro phosphorylation assays were performed in HEK293 cells as described above. In this case, we tested rGSK3β and recombinant *X. laevis* PKCα (rPKCα) on Aqp8bb-Flag-WT and mutant channels, in which Aqp8bb Ser^{14} (salmon) or Ser^{16} (zebrafish) were replaced by Ala. Immunoblot results showed that salmon Aqp8bb-Flag-WT was equally phosphorylated by rPKCα and rGSK3β at Ser residues, whereas rGSK3β was no longer able to phosphorylate Ser residues

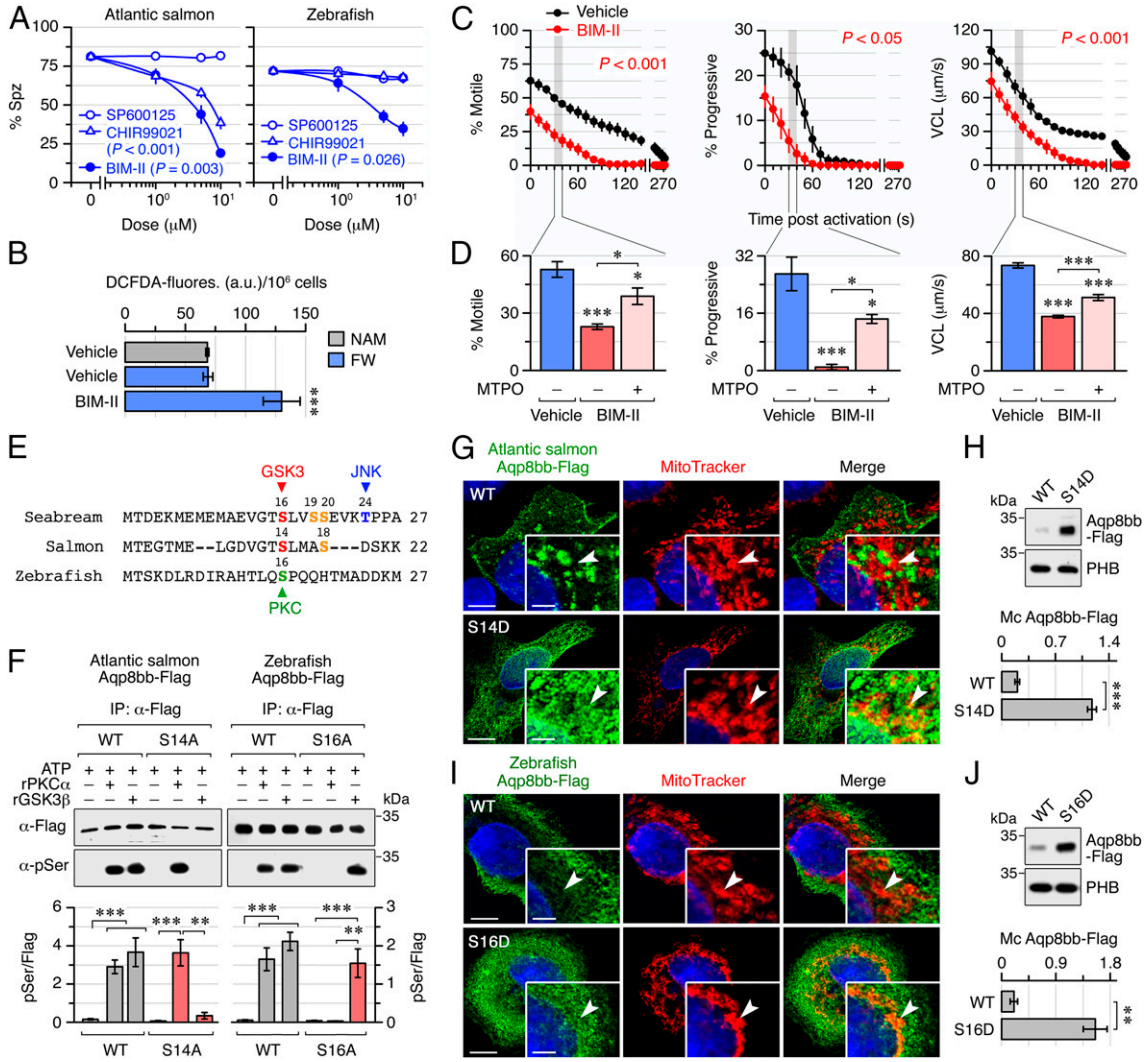

Fig. 7. Aqp8bb mitochondrial transport in FW spermatozoa is controlled by monophosphorylation of the N terminus of the channel by PKC or GSK3. (*A*) Percentage of salmon and zebrafish spermatozoa (mean ± SEM; $n = 4$ fish for salmon, and $n = 3$ pools of 5 fish for zebrafish) showing Aqp8bb mitochondrial localization after treatment with vehicle (DMSO), or JNK (SP600125), PKC (BIM-II), or GSK3 (CHIR99021) inhibitors. (*B*) ROS levels (mean ± SEM; $n = 6$ fish) in immotile and activated zebrafish spermatozoa treated with vehicle or BIM-II. (*C*) Motility, progressivity, and VCL of zebrafish activated spermatozoa (mean ± SEM, $n = 7$ fish) treated with vehicle or BIM-II. *P* values are calculated from the Mann–Whitney *U* test (during the first 60 s only for motility and progressivity). (*D*) Effect of MTPO (50 μM) on BIM-II inhibition of zebrafish sperm kinetics (mean ± SEM, $n = 5$ fish) at 30 to 40 s postactivation (gray bar in *C*). Data in *B* and *D* are statistically analyzed by one-way ANOVA (***$P < 0.001$; *$P < 0.05$, with respect to nontreated sperm). (*E*) Amino acid sequence alignment of seabream, salmon, and zebrafish Aqp8bb N terminus indicating the GSK3, PKC, and JNK phosphorylation sites. (*F*) Immunoblot of Ser phosphorylation in salmon and zebrafish Aqp8bb-Flag-WT and -S14A and -S16A mutants, respectively, after phosphorylation in vitro by rPKCα (0.08 μM) and rGSK3β (0.17 μM). (*Lower*) Quantitation of phosphorylated channel normalized to total immunoprecipitated protein. (*G* and *I*) Aqp8bb-Flag and MTR double staining of HepG2 cells expressing salmon (*G*) or zebrafish (*I*) Aqp8bb-Flag-WT and phosphomimetic mutants. Arrowheads indicate colocalized signals in the mitochondria. (Scale bars, 10 μm; *Insets*, 5 μm.) (*H* and *J*) Immunoblots of Aqp8bb-Flag-WT and mutants in mitochondrial extracts from cells shown in *G* and *I*. Data in *F*, *H*, and *J* are the mean ± SEM of three separate experiments, and are statistically analyzed by one-way ANOVA (*F*) or an unpaired Student's *t* test (*H* and *J*). ***$P < 0.001$; **$P < 0.01$, as indicated in brackets.

in the Aqp8bb-Flag-S14A mutant, and only Ser phosphorylation by rPKCα was detected (Fig. 7*F*). Similarly, zebrafish Aqp8bb-Flag-WT was Ser-phosphorylated by rPKCα and rGSK3β, but the Aqp8b-Flag-S16A mutant could only be phosphorylated by rGSK3β (Fig. 7*F*). These data indicate that salmon Aqp8bb Ser^{14} and zebrafish Aqp8bb Ser^{16} are, respectively, the target residues of rGSK3β, and rPKCα. However, both salmon and zebrafish channels contain other residues that are phosphorylated by rPKCα and rGSK3β, respectively.

Finally, we transiently expressed salmon and zebrafish Aqp8bb-Flag-WT in HepG2 cells and determined the effect of external Ca^{2+} and/or H_2O_2 on mitochondrial channel localization. In contrast to seabream, Aqp8bb immunostaining of MTR-loaded cells, as well as immunoblotting of mitochondrial extracts, showed that only Ca^{2+} was able to traffic both salmon and zebrafish Aqp8bb-Flag-WT to the mitochondria (*SI Appendix*, Fig. S10 *A* and *B*). Since Ser^{14} and Ser^{16} from salmon and zebrafish Aqp8bb are, respectively, the target sites of Ca^{2+}-activated GSK3 and PKC, we investigated whether phosphomimetic mutations at these sites could induce mitochondrial targeting of the channels. For salmon Aqp8bb, we also tested Ser^{20} in case this residue could play a role as a priming site for GSK3 phosphorylation. All constructs were expressed at similar levels in HepG2 cells (*SI Appendix*, Fig. S10 *C* and *D*), but immunostaining and immunoblotting data indicated that only the salmon Aqp8bb-Flag-S14D and zebrafish Aqp8bb-Flag-S16D mutants were constitutively targeted to the

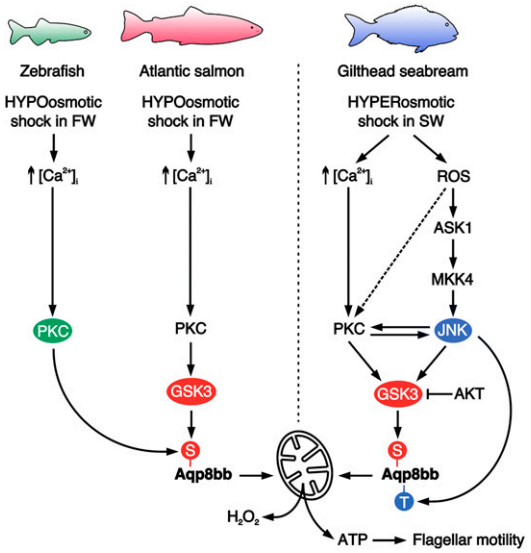

Fig. 8. A model for the evolution of the intracellular multiplier peroxiporin signal transduction pathway powering piscine spermatozoa. In spermatozoa from more primitive FW teleost lineages, such as in zebrafish and salmonids, a rise of intracellular Ca^{2+} ($[Ca^{2+}]_i$) upon activation in FW triggers the PKC-GSK3 signaling pathway, leading to the direct PKC (zebrafish) or GSK3 (Atlantic salmon) phosphorylation of N-terminal Aqp8bb residues, promoting rapid channel trafficking to the mitochondria. In modern marine teleosts such as the seabream, which release the sperm into SW, a cross-talk between $[Ca^{2+}]_i$-activated PKC and ROS-activated JNK and PKC signaling pathways converge to activate GSK3 with an additional JNK-mediated multiplier regulation of Aqp8bb mitochondrial trafficking to cope with a higher osmotic stress.

mitochondria (Fig. 7 *G–J* and *SI Appendix*, Fig. S10*C*). Taken together, these data suggest that Ca^{2+}-activated PKC or the PKC/GSK3 cascade are the effective pathways phosphorylating Ser^{16} or Ser^{14} in the N terminus of zebrafish and salmon Aqp8bb, respectively, which traffic the peroxiporin to the mitochondria.

Discussion

The present work reveals insight into the evolution of molecular mechanisms regulating spermatozoan kinematic properties in an infraclass of vertebrates that display intense levels of sperm competition. The data show that the rapid mitochondrial trafficking of an Aqp8bb peroxiporin, first discovered in a marine teleost (26), is consistently regulated through N-terminal phosphorylation in FW and SW teleosts. Such channel regulation thus represents a conserved mechanism of mitochondrial ROS detoxification for the maintenance of ATP production and improved spermatozoon performance.

The model arising from the data (Fig. 8) suggests that the signal transduction pathways regulating Aqp8bb trafficking in teleost spermatozoa evolved increasing levels of sophistication and cross-talk between the pathways through the inclusion of alternative kinase cascade modules. Thus, in older lineages of FW teleost in which spermatozoon motility is activated through hypoosmotic shock, a more direct Ca^{2+}-PKC–mediated pathway phosphorylating the Aqp8bb N terminus suffices (Fig. 8). However, in the protacanthopterygian FW salmonids, in which the importance of sperm velocity under sperm competition is well known (50), a PKC-regulated GSK3 cascade is added and the channel is only phosphorylated by GSK3 to induce its trafficking (Fig. 8). The addition of the extra GSK3 regulatory layer may act as a multiplier if the expression levels of this kinase significantly exceed those of PKC, a facet that could explain the higher sperm velocities of sedentary parasitic males compared to anadromous "bourgeois" males (51). In contrast to the FW species, we find that marine spermatozoa have recruited an addtitional ROS-triggered JNK pathway to cope with the elevated hypertonic stress (Fig. 8). In this case, JNK directly activates GSK3, but also cross-talks with Ca^{2+}- and ROS-activated PKC to trigger Aqp8bb N-terminal phosphorylation by GSK3, thus creating a multiplier pathway for the regulation of the peroxiporin trafficking. In addition, JNK bypasses the GSK3 pathway to directly phosphorylate the channel in a different N-terminal residue, further enhancing the peroxiporin trafficking.

The conserved action of PKC in each of the pathways regulating Aqp8bb trafficking in FW and SW spermatozoa reveals how the multiplier mechanism evolved. In SW-activated spermatozoa, both Ca^{2+} and ROS induce PKC activity, with ROS also inducing JNK activity through the ASK1-MKK4 cascade to further enhance PKC catalysis which, together with the direct activation of GSK3 by JNK, multiplies the action of GSK3 to phosphorylate Aqp8bb (Fig. 8). The importance of this stress-induced multiplier pathway is clearly evident on the spermatozoon kinematic properties, where JNK inhibition more rapidly suppresses the degree of motility, progressivity and velocity of spermatozoa compared to GSK3 inhibition. Consequently, it seems likely that positive selection of the JNK pathway with efficient catalytic kinetics would be advantageous in the sperm competition of SW species, while those of the PKC and GSK3 pathways would be favorable for FW species.

Interestingly, with the exception of the cross-talk between JNK and PKC to activate GSK3, we were able to replicate the signaling pathways regulating mitochondrial Aqp8bb trafficking in piscine spermatozoa in human cells. This finding suggests that these signal-transduction pathways are ancient and were likely present in the last common ancestor of mammals and fishes (>435 million y ago) (52). However, although ROS transport is involved in normal human spermatozoa functioning, and AQP8 has been observed in the midpiece and likely in the mitochondria (53, 54), it is not yet clear whether AQP8 functions as a mitochondrial peroxiporin in mammalian sperm. If indeed AQP8 is an orthologous mitochondrial peroxiporin contributing to the kinematic properties of vertebrate spermatozoa, it will be revealing to identify whether the same JNK and GSK3 pathways are involved in AQP8 trafficking mechanisms.

In mammals, the Ser/Thr kinase GSK3 is encoded by two paralogous genes (*GSK3α* and *GSK3β*), the activities of which are regulated by posttranslational Ser^{21}/Ser^{9} and Tyr^{279}/Tyr^{216} phosphorylation (37). It is now well recognized that the GSK3α enzyme plays an important role in the acquisition of sperm motility and acrosomal reaction in mammals (55–57). The inhibitory $GSK3\alpha^{S21}$ phoshorylation is high during the epididymal sperm maturation stage, but subsequently decreases to activate the kinase activity during the hyperactivation phase in the female oviduct (58–61). This latter mammalian hyperactivation mechanism is reminiscent of the activation of motility in marine fish spermatozoa (31), which is also associated with the dephosphorylation of $GSK3\alpha^{S21}$ as demonstrated here in the seabream. In teleosts, however, the role of GSK3 on spermatozoon function has remained largely unknown, although a recent study in zebrafish has shown that the knockout of miR-34a, which normally down-regulates GSK3, enhances sperm motility and the fertilization rates (62). Since we show that GSK3 is not involved in the peroxiporin trafficking mechanism in zebrafish spermatozoa, it seems likely that this kinase controls other elements of the motility. Indeed, the inability of the antioxidant mito-TEMPO to rescue seabream spermatozoa motility, when inhibited by the GSK3 blocker CHIR99021, supports the notion that GSK3 plays additional motility activation roles unrelated to Aqp8bb mitochondrial detoxification.

In contrast to GSK3, the role of the stress-activated JNK cascade for spermatozoon motility in vertebrates is less well known. This pathway is involved in both proapoptotic and antiapoptotic

mechanisms in response to various stimuli, such as osmotic and oxidative stress (63). The data available for mammalian spermatozoa suggest a role for JNK in cell survival under osmotic stress (64), as well as during progesterone-induced hyperactivation (65). Such a role of JNK during osmotic stress is consistent with the results of the present study showing the involvement of the JNK signaling pathway controlling Aqp8bb-mediated mitochondrial detoxification in marine spermatozoa. Interestingly, in the nonflagelated spermatozoa of the nematode *Caenorhabditis elegans*, both Ca^{2+} and the MAPK cascade, which functions downstream of, or parallel with, the Ca^{2+} signaling, are necessary for sperm activation (66). This resembles the molecular scenario controlling Aqp8bb trafficking in seabream spermatozoa. In addition, pharmacological activation of JNK/p38 MAPK is sufficient to trigger sperm motility acquisition in *C. elegans* (66), while the same treatment of immotile seabream sperm bypasses the requirement of the Ca^{2+} signal for the induction of mitochondrial Aqp8bb transport. Therefore, although nematode and fish spermatozoa are morphologically distinct, and their motility is regulated by different molecular machineries, both types of spermatozoa appear to utilize conserved signaling pathways for different purposes, to modulate sperm maturation in the case of the nematode, or to insert a peroxiporin in the mitochondrion of the seabream spermatozoon as an antiapoptotic mechanism.

Our pharmacological studies in seabream sperm and HepG2 cells suggest a complex cascade of kinase phosphorylation events, where PKC- and JNK-mediate GSK3 activation by GSK3α/$\beta^{Y279/216}$ phosphorylation, and PKC activates JNK and vice versa. However, both PKC and JNK are Ser/Thr kinases, and in ejaculated mammalian spermatozoa PKC inhibits, rather than activates, GSK3 activity by GSK3α^{S21} inhibitory phosphorylation (67–69). In contrast, in colon cancer cells the atypical PKCζ isoform can rapidly and transiently activate GSK3β activity through Ser^{147} phosphorylation, which is also required to maintain the constitutive basal activity of GSK3β (69). Although a PKCζ ortholog is expressed in fish sperm (70), the role of this specific kinase regulating GSK3 and Aqp8bb mitochondrial transport requires further investigation. The PKC-mediated GSK3α$\beta^{Y279/216}$ phosphorylation occurring in seabream sperm could also be an indirect mechanism, as it seems to occur during the activation of GSK3 by JNK, or the activation of JNK by PKC. The latter would resemble the Toll-like receptor 4 transient receptor potential channel 1-PKCα signaling pathway that is triggered as defense and proinflammatory response to bacterial infection (71), in which PKC may phosphorylate Ser^{129} in JNK augmenting its phosphorylation by MKK4 (72). The JNK-mediated activation of GSK3 has been reported to take place in a hepatocyte cell line through the MAP3K mixed-lineage kinase 3 in a positive feedback mechanism (73). A similar indirect mechanism mediating the activation of GSK3 by JNK might occur through stimulation of the proline-rich tyrosine kinase 2, which is a Ca^{2+}-activated tyrosine kinase in capacitated human sperm (74), or through the Src-related tyrosine kinase Fyn (75).

The present study provides evidence suggesting that piscine Aqp8bb is a physiological substrate of PKC, GSK3, and JNK, which regulate channel trafficking. This is supported by the demonstration that these kinases can phosphorylate the different teleost Aqp8bb orthologs in vitro, and that mutations of the respective target sites trigger or abolish mitochondrial channel transport. In the seabream model, it is also supported by the observation that inhibition of GSK3 and JNK activity through the expression of dominant-negative forms of the kinases in HepG2 cells specifically reduces the phosphorylation of the target sites in the channel and impairs mitochondrial trafficking. The phosphorylation of Aqp8bb by JNK at Thr^{24} could play a role as a priming mechanism for subsquent GSK3 phosphorylation since our in vitro data show that mimicking a constitutive phosphorylated state of this site can enhance GSK3 phosphorylation of Ser^{16} in the channel. This would agree with the observation that under cell stress JNK can phosphorylate antiapoptotic proteins priming them for subsequent phosphorylation by GSK3 (45). However, we found that mutation of Thr^{24} into Ala in seabream Aqp8bb to prevent its phosphorylation by JNK does not reduce GSK3-mediated Ser phosphorylation of the channel in HepG2 cells during Ca^{2+} and H_2O_2 stimulation. This therefore argues against a role of JNK as a priming kinase for GSK3. Rather, our data indicate that GSK3 and JNK phosphorylation of Aqp8bb are both required for maximum accumulation of the channel in the mitochondria.

In summary, this work presents a mechanism of spermatozoon motility regulation in animals. The data show that a conserved process of mitochondrial ROS detoxification evolved in piscine spermatozoa to enhance their kinematic properties. The detoxification process occurs through the rapid trafficking of an Aqp8bb peroxiporin to the inner mitochodrial membrane to facilitate H_2O_2 efflux and the continued production of ATP necessary for flagellar contractions. The signal transduction cascades controlling the trafficking mechanism are rapidly activated in ejaculated sperm through hydration in FW teleosts and dehydration in SW teleosts, leading to phosphorylation of Ser/Thr residues in the Aqp8bb N terminus. The data further reveal the evolution of an increasingly sophisticated hierarchy of kinases activating the trafficking mechanism with more direct Ca^{2+}-PKC or Ca^{2+}-PKC-GSK3 induction pathways in ancient lineages of FW teleosts to a cross-talk between the Ca^{2+}-PKC-GSK3 signaling mechanism and a ROS-activated JNK multiplier pathway in modern lineages of marine teleosts. These findings uncover gene networks involved in postactivated spermatozoon swimming performance and thus provide insight into the molecular controls that may form selective traits for postcopulatory sexual selection.

Materials and Methods

Detailed information on the methods employed are provided in *SI Appendix, Supplementary Materials and Methods*.

Procedures relating to the care and use of animals and sample collection were approved by the Ethics Committee of the Institute of Agrifood Research and Technology, following the European Union Council Guidelines (86/609/EU), or in accordance with the regulations approved by the governmental Norwegian Animal Research Authority (http://www.fdu.no/fdu/).

Data Availability. All study data are included in the article and *SI Appendix*.

ACKNOWLEDGMENTS. We thank Prof. S. S. Madsen for providing Atlantic salmon Aqp8aa, -8ab, and -8bb specific antibodies. This work was supported by Spanish Ministry of Economy, Industry and Competitiveness (MINECO) Grant AGL2016-76802-R (to J.C.) and Norwegian Research Council Grants 254872/E40 and 294768/E40 (to R.N.F.). F.C. and A.F. were supported, respectively, by a "Ramon y Cajal" contract (RYC-2015-17103) and a predoctoral grant (BES-2014-068745) from Spanish MINECO.

1. M. J. Gage, P. Stockley, G. A. Parker, Effects of alternative male mating strategies on characteristics of sperm production in the Atlantic salmon (*Salmo salar*): Theoretical and empirical investigations. *Philos. Trans. R. Soc. Lond. B Biol. Sci.* **350**, 391–399 (1995).
2. D. P. Froman, A. J. Feltmann, M. L. Rhoads, J. D. Kirby, Sperm mobility: A primary determinant of fertility in the domestic fowl (*Gallus domesticus*). *Biol. Reprod.* **61**, 400–405 (1999).
3. E. Kupriyanova, J. N. Havenhand, Variation in sperm swimming behaviour and its effect on fertilization success in the serpulid polychaete *Galeolaria caespitosa*. *Invertebr. Reprod. Dev.* **41**, 21–26 (2002).
4. T. Pizzari, G. A. Parker, "Sperm competition and sperm phenotype" in *Sperm Biology: An Evolutionary Perspective*, T. R. Birkhead, D. J. Hosken, S. Pitnick, Eds. (Academic Press, 2009), pp. 207–245.
5. E. Del Olmo *et al.*, Fertility of cryopreserved ovine semen is determined by sperm velocity. *Anim. Reprod. Sci.* **138**, 102–109 (2013).
6. R. K. Browne *et al.*, Sperm motility of externally fertilizing fish and amphibians. *Theriogenology* **83**, 1–13 (2015).
7. A. M. Cancel, D. Lobdell, P. Mendola, S. D. Perreault, Objective evaluation of hyperactivated motility in rat spermatozoa using computer-assisted sperm analysis. *Hum. Reprod.* **15**, 1322–1328 (2000).

8. D. R. Levitan, Sperm velocity and longevity trade off each other and influence fertilization in the sea urchin Lytechinus variegatus. *Proc. Biol. Sci.* **267**, 531–534 (2000).
9. T. R. Birkhead, F. M. Hunter, Mechanisms of sperm competition. *Trends Ecol. Evol.* **5**, 48–52 (1990).
10. M. J. Gage *et al*., Spermatozoal traits and sperm competition in Atlantic salmon: Relative sperm velocity is the primary determinant of fertilization success. *Curr. Biol.* **14**, 44–47 (2004).
11. S. Liljedal, G. Rudolfsen, I. Foldstad, Factors predicting male fertilization success in an external fertilizer. *Behav. Ecol. Sociobiol.* **62**, 1805–1811 (2008).
12. J. L. Fitzpatrick *et al*., Female promiscuity promotes the evolution of faster sperm in cichlid fishes. *Proc. Natl. Acad. Sci. U.S.A.* **106**, 1128–1132 (2009).
13. C. Gasparini, L. W. Simmons, M. Beveridge, J. P. Evans, Sperm swimming velocity predicts competitive fertilization success in the green swordtail *Xiphophorus helleri*. *PLoS One* **5**, e12146 (2010).
14. C. Boschetto, C. Gasparini, A. Pilastro, Sperm number and velocity affect sperm competition success in the guppy (*Poecilia reticulata*). *Behav. Ecol. Sociobiol.* **65**, 813–821 (2011).
15. M. Tourmente, M. Gomendio, E. R. Roldan, Sperm competition and the evolution of sperm design in mammals. *BMC Evol. Biol.* **11**, 12 (2011).
16. G. A. Parker, Sperm competition and its evolutionary consequences in the insects. *Biol. Rev. Camb. Philos. Soc.* **45**, 525–567 (1970).
17. G. A. Parker, T. Pizzari, Sperm competition and ejaculate economics. *Biol. Rev. Camb. Philos. Soc.* **85**, 897–934 (2010).
18. P. Stockley, M. J. G. Gage, G. A. Parker, A. P. Møller, Sperm competition in fishes: The evolution of testis size and ejaculate characteristics. *Am. Nat.* **149**, 933–954 (1997).
19. A. Civetta, J. M. Ranz, Genetic factors influencing sperm competition. *Front. Genet.* **10**, 820 (2019).
20. R. C. Firman, L. W. Simmons, Sperm midpiece length predicts sperm swimming velocity in house mice. *Biol. Lett.* **6**, 513–516 (2010).
21. T. V. Vladić, B. A. Afzelius, G. E. Bronnikov, Sperm quality as reflected through morphology in salmon alternative life histories. *Biol. Reprod.* **66**, 98–105 (2002).
22. S. Lüpold, S. Calhim, S. Immler, T. R. Birkhead, Sperm morphology and sperm velocity in passerine birds. *Proc. Biol. Sci.* **276**, 1175–1181 (2009).
23. E. de Lamirande, C. Gagnon, Reactive oxygen species and human spermatozoa. I. Effects on the motility of intact spermatozoa and on sperm axonemes. *J. Androl.* **13**, 368–378 (1992).
24. E. de Lamirande, C. Gagnon, Reactive oxygen species and human spermatozoa. II. Depletion of adenosine triphosphate plays an important role in the inhibition of sperm motility. *J. Androl.* **13**, 379–386 (1992).
25. J. S. Armstrong *et al*., Characterization of reactive oxygen species induced effects on human spermatozoa movement and energy metabolism. *Free Radic. Biol. Med.* **26**, 869–880 (1999).
26. F. Chauvigné, M. Boj, R. N. Finn, J. Cerdà, Mitochondrial aquaporin-8-mediated hydrogen peroxide transport is essential for teleost spermatozoon motility. *Sci. Rep.* **5**, 7789 (2015).
27. S. Sadeghi *et al*., Effect of different oxidative stress degrees generated by hydrogen peroxide on motility and DNA fragmentation of zebrafish (*Danio rerio*) spermatozoa. *Reprod. Domest. Anim.* **53**, 1498–1505 (2018).
28. L. Burnaugh, B. A. Ball, K. Sabeur, A. D. Thomas, S. A. Meyers, Osmotic stress stimulates generation of superoxide anion by spermatozoa in horses. *Anim. Reprod. Sci.* **117**, 249–260 (2010).
29. R. N. Finn, F. Chauvigné, J. B. Hlidberg, C. P. Cutler, J. Cerdà, The lineage-specific evolution of aquaporin gene clusters facilitated tetrapod terrestrial adaptation. *PLoS One* **9**, e113686 (2014).
30. E. Koren, J. Lukac, Mechanism of liquefaction of the human ejaculate. I. Changes of the ejaculate proteins. *J. Reprod. Fertil.* **56**, 493–499 (1979).
31. J. Cosson *et al*., Marine fish spermatozoa: Racing ephemeral swimmers. *Reproduction* **136**, 277–294 (2008).
32. J. Cosson, "Fish sperm physiology: Structure, factors regulating motility, and motility evaluation" in *Biological Research in Aquatic Science*, Y. Bozkurt, Ed. (IntechOpen, 2019), 10.5772/intechopen.85139.
33. G. N. Cherr *et al*., Two egg-derived molecules in sperm motility initiation and fertilization in the Pacific herring (*Clupea pallasi*). *Int. J. Dev. Biol.* **52**, 743–752 (2008).
34. R. J. Davis, Signal transduction by the JNK group of MAP kinases. *Cell* **103**, 239–252 (2000).
35. M. Yan *et al*., Activation of stress-activated protein kinase by MEKK1 phosphorylation of its activator SEK1. *Nature* **372**, 798–800 (1994).
36. E. H. Goldman, L. Chen, H. Fu, Activation of apoptosis signal-regulating kinase 1 by reactive oxygen species through dephosphorylation at serine 967 and 14-3-3 dissociation. *J. Biol. Chem.* **279**, 10442–10449 (2004).
37. E. Beurel, S. F. Grieco, R. S. Jope, Glycogen synthase kinase-3 (GSK3): Regulation, actions, and diseases. *Pharmacol. Ther.* **148**, 114–131 (2015).
38. D. R. Alessi, A. Cuenda, P. Cohen, D. T. Dudley, A. R. Saltiel, PD 098059 is a specific inhibitor of the activation of mitogen-activated protein kinase kinase in vitro and in vivo. *J. Biol. Chem.* **270**, 27489–27494 (1995).
39. A. P. Kozikowski, H. Sun, J. Brognard, P. A. Dennis, Novel PI analogues selectively block activation of the pro-survival serine/threonine kinase Akt. *J. Am. Chem. Soc.* **125**, 1144–1145 (2003).
40. S. F. Moore *et al*., Dual regulation of glycogen synthase kinase 3 (GSK3)α/β by protein kinase C (PKC)α and Akt promotes thrombin-mediated integrin αIIbβ3 activation and granule secretion in platelets. *J. Biol. Chem.* **288**, 3918–3928 (2013).
41. M. Boj, F. Chauvigné, J. Cerdà, Coordinated action of aquaporins regulates sperm motility in a marine teleost. *Biol. Reprod.* **93**, 40 (2015).
42. A. Matsuzawa, H. Ichijo, Redox control of cell fate by MAP kinase: Physiological roles of ASK1-MAP kinase pathway in stress signaling. *Biochim. Biophys. Acta* **1780**, 1325–1336 (2008).
43. M. Hagedorn, M. McCarthy, V. L. Carter, S. A. Meyers, Oxidative stress in zebrafish (*Danio rerio*) sperm. *PLoS One* **7**, e39397 (2012).
44. Y. Li, M. A. Trush, Diphenyleneiodonium, an NAD(P)H oxidase inhibitor, also potently inhibits mitochondrial reactive oxygen species production. *Biochem. Biophys. Res. Commun.* **253**, 295–299 (1998).
45. C. Sutherland, What are the bona fide GSK3 Substrates? *Int. J. Alzheimers Dis.* **2011**, 505607 (2011).
46. X. Ren, X. Chen, Z. Wang, D. Wang, Is transcription in sperm stationary or dynamic? *J. Reprod. Dev.* **63**, 439–443 (2017).
47. M. J. Marchissio, D. E. Francés, C. E. Carnovale, R. A. Marinelli, Mitochondrial aquaporin-8 knockdown in human hepatoma HepG2 cells causes ROS-induced mitochondrial depolarization and loss of viability. *Toxicol. Appl. Pharmacol.* **264**, 246–254 (2012).
48. V. F. Taelman *et al*., Wnt signaling requires sequestration of glycogen synthase kinase 3 inside multivesicular endosomes. *Cell* **143**, 1136–1148 (2010).
49. B. Dérijard *et al*., JNK1: A protein kinase stimulated by UV light and Ha-Ras that binds and phosphorylates the c-Jun activation domain. *Cell* **76**, 1025–1037 (1994).
50. J. Beirão, T. B. Egeland, C. F. Purchase, J. T. Nordeide, Fish sperm competition in hatcheries and between wild and hatchery origin fish in nature. *Theriogenology* **133**, 201–209 (2019).
51. M. Taborsky, Sperm competition in fish: 'Bourgeois' males and parasitic spawning. *Trends Ecol. Evol.* **13**, 222–227 (1998).
52. S. Kumar, G. Stecher, M. Suleski, S. B. Hedges, TimeTree: A resource for timelines, timetrees, and divergence times. *Mol. Biol. Evol.* **34**, 1812–1819 (2017).
53. U. Laforenza *et al*., Aquaporin-mediated water and hydrogen peroxide transport is involved in normal human spermatozoa functioning. *Int. J. Mol. Sci.* **18**, 66 (2016).
54. G. Pellavio *et al*., HPV infection affects human sperm functionality by inhibition of Aquaporin-8. *Cells* **9**, 1241 (2020).
55. R. Bhattacharjee *et al*., Targeted disruption of glycogen synthase kinase 3A (GSK3A) in mice affects sperm motility resulting in male infertility. *Biol. Reprod.* **92**, 65 (2015).
56. A. T. Reid *et al*., Glycogen synthase kinase 3 regulates acrosomal exocytosis in mouse spermatozoa via dynamin phosphorylation. *FASEB J.* **29**, 2872–2882 (2015).
57. S. Dey *et al*., Roles of glycogen synthase kinase 3 alpha and calcineurin in regulating the ability of sperm to fertilize eggs. *FASEB J.* **34**, 1247–1269 (2020).
58. S. Koch, S. P. Acebron, J. Herbst, G. Hatiboglu, C. Niehrs, Post-transcriptional Wnt signaling governs epididymal sperm maturation. *Cell* **163**, 1225–1236 (2015).
59. M. J. Freitas *et al*., Isoform-specific GSK3A activity is negatively correlated with human sperm motility. *Mol. Hum. Reprod.* **25**, 171–183 (2019).
60. S. Dey, C. Brothag, S. Vijayaraghavan, Signaling enzymes required for sperm maturation and fertilization in mammals. *Front. Cell Dev. Biol.* **7**, 341 (2019).
61. D. Martin-Hidalgo, R. Serrano, C. Zaragoza, L. J. Garcia-Marin, M. J. Bragado, Human sperm phosphoproteome reveals differential phosphoprotein signatures that regulate human sperm motility. *J. Proteomics* **215**, 103654 (2020).
62. W. Guo *et al*., miR-34a regulates sperm motility in zebrafish. *Int. J. Mol. Sci.* **18**, 2676 (2017).
63. J. Yue, J. M. López, Understanding MAPK signaling pathways in apoptosis. *Int. J. Mol. Sci.* **21**, 2346 (2020).
64. B. M. García *et al*., The mitochondria of stallion spermatozoa are more sensitive than the plasmalemma to osmotic-induced stress: Role of c-Jun N-terminal kinase (JNK) pathway. *J. Androl.* **33**, 105–113 (2012).
65. V. Sagare-Patil *et al*., Differential concentration and time dependent effects of progesterone on kinase activity, hyperactivation and acrosome reaction in human spermatozoa. *Int. J. Androl.* **35**, 633–644 (2012).
66. Z. Liu, B. Wang, R. He, Y. Zhao, L. Miao, Calcium signaling and the MAPK cascade are required for sperm activation in *Caenorhabditis elegans*. *Biochim. Biophys. Acta* **1843**, 299–308 (2014).
67. I. M. Aparicio *et al*., Porcine sperm motility is regulated by serine phosphorylation of the glycogen synthase kinase-3alpha. *Reproduction* **134**, 435–444 (2007).
68. M. J. Bragado, I. M. Aparicio, M. C. Gil, L. J. Garcia-Marin, Protein kinases A and C and phosphatidylinositol 3 kinase regulate glycogen synthase kinase-3A serine 21 phosphorylation in boar spermatozoa. *J. Cell. Biochem.* **109**, 65–73 (2010).
69. N. Tejeda-Muñoz, H. González-Aguilar, P. Santoyo-Ramos, M. C. Castañeda-Patlán, M. Robles-Flores, Glycogen synthase kinase 3β is positively regulated by protein kinase Cζ-mediated phosphorylation induced by Wnt agonists. *Mol. Cell. Biol.* **36**, 731–741 (2015).
70. C. F. Huang, H. C. Chen, N. N. Chuang, C. M. Kuo, The zeta protein kinase C isoform from the testis of the grey mullet *Mugil cephalus* with a specific reaction protein of M(r) 48,000 on oolemma. *Comp. Biochem. Physiol. C Pharmacol. Toxicol. Endocrinol.* **111**, 429–433 (1995).
71. X. Zhou *et al*., Transient receptor potential channel 1 deficiency impairs host defense and proinflammatory responses to bacterial infection by regulating protein kinase Cα signaling. *Mol. Cell. Biol.* **35**, 2729–2739 (2015).
72. P. López-Bergami *et al*., RACK1 mediates activation of JNK by protein kinase C [corrected]. *Mol. Cell* **19**, 309–320 (2005).
73. M. Sharma, V. Gadang, A. Jaeschke, Critical role for mixed-lineage kinase 3 in acetaminophen-induced hepatotoxicity. *Mol. Pharmacol.* **82**, 1001–1007 (2012).
74. N. G. Brukman *et al*., Tyrosine phosphorylation signaling regulates Ca^{2+} entry by affecting intracellular pH during human sperm capacitation. *J. Cell. Physiol.* **234**, 5276–5288 (2019).
75. M. Lesort, R. S. Jope, G. V. Johnson, Insulin transiently increases tau phosphorylation: Involvement of glycogen synthase kinase-3beta and Fyn tyrosine kinase. *J. Neurochem.* **72**, 576–584 (1999).